A Current-Based Algorithm for the Design of Metasurface Antennas

A Current-Based Algorithm for the Design of Metasurface Antennas

Marcello Zucchi*, Francesco Vernì*, Marco Righero†, Giuseppe Vecchi*
*Department of Electronics and Telecommunications, Politecnico di Torino, Turin, Italy, marcello.zucchi@polito.it
†Advanced Computing, Photonics & Electromagnetics (CPE), Fondazione LINKS, Turin, Italy

***Abstract*—This paper proposes an algorithm for the automated design of metasurface antennas. From the objective radiation field and the feeding structure, it allows to obtain a surface current distribution that leads to a passive and lossless impedance profile on the radiating aperture. The surface is modelled by a scalar impedance boundary condition and the electromagnetic problem is formulated as an electric field integral equation. The approach is entirely numerical, based on the gradient descent optimization of a scalar objective function that incorporates passivity and far field requirements. This procedure was applied to the design of an electrically large circular metasurface antenna at 32 GHz, obtaining a lossless impedance profile with satisfactory radiation properties.**

***Index Terms*—antenna optimization, metasurface antennas, method of moments (MoM), impedance boundary condition (IBC).**

I. Introduction

In recent years, Metasurface antennas (MTS) have represented one of the most promising technology for the realization of low-profile antennas, mainly due to their attracting properties in terms of low losses and simple manufacturing [1]. They are based on a patterned radiating surface which is excited by a single source. The patterning, made of sub-wavelength conducting patches over a grounded dielectric slab, determines the radiation properties of the antenna.

The main challenge in their design is the presence of multi-scale features: the large electrical size of the radiating aperture is contrasted by the small details of the patterning. A direct optimization is therefore unfeasible from the computational point of view, and the process is usually split in two consecutive steps: 1) design of a continuous impedance profile that yields the expected radiation performance, and 2) implementation of the resulting profile by means of suitably shaped metallic cells printed on a grounded substrate. We will focus on the first step, while the second part is typically carried out by means of established procedures [2].

Different methods have been proposed for the design of these type of antennas. Some of them employ analytical approximations of the impedance in the design of spiral leaky-wave antennas [3], while others rely on a numerical approach with a full wave solution based on entire-domain basis functions for the synthesis of circular metasurface antennas [4], [5]. A somewhat related numerical inversion methodology has been applied to the design of metasurface screens, with power conservation explicitly enforced [6], [7]. Lastly, in [8], an alternated projection algorithm has been proposed which directly enforces the passivity of the resulting impedance. All these methods are based on the direct synthesis of the impedance profile. However, their formulation applies only to specific geometries.

The present paper presents an alternative approach that focuses on the optimization of the equivalent surface current. The problem is formulated as the unconstrained minimization of a differentiable scalar objective function which takes into account both requirements of local passivity and objective radiation field. A gradient-based solution is sought for, with a formulation that allows to accelerate the gradient computation by means of fast algorithms commonly used in the solution of MoM linear systems and far field computation.

II. Synthesis of Metasurface Antennas

A. Impedance Boundary Condition

Metasurface antennas can be modeled macroscopically by means of an infinitely thin layer of penetrable surface impedance over a dielectric grounded substrate. Its behaviour is represented locally by a scalar Impedance Boundary Condition (IBC), which relates the tangential electric field to the jump of the tangential magnetic field across the layer:

$$\boldsymbol{E}_{\mathrm{t}} = Z_{\mathrm{s}}\, \hat{\boldsymbol{n}} \times \left(\boldsymbol{H}^{+} - \boldsymbol{H}^{-} \right) = Z_{\mathrm{s}}\, \boldsymbol{J}_{\mathrm{s}}, \tag{1}$$

where $\boldsymbol{J}_{\mathrm{s}}$ is the equivalent surface electric current. This formulation leads to a stable numerical scheme when solved, together with the Electric Field Integral Equation (EFIE-IBC), with the Method of Moments [9].

The impedance is required to be locally passive and lossless in order for it to be practically realizable with metallic patches. This constrains impedance values to be purely imaginary.

B. Numerical Algorithm

The algorithm starts with the discretization of the radiating surface with a triangular mesh. The equivalent surface current is represented as a linear combination of Rao-Wilton-Glisson (RWG) basis functions. The setup phase is completed with the computation and storage of the information needed for the solution of the EFIE-IBC linear system. In particular, the combined effect of the dielectric substrate and of the ground plane is taken into account inside the Green's function employed in the MoM solution.

The procedure is outlined by the following steps:

1) choice of the initial current,

2) optimization of the objective function given the far field requirement and the source field, in order to find the optimum current,
3) computation of the impedance from the knowledge of the source field and of the optimized current.

Since a gradient-based solution is inherently local, the choice of the initial current is key to obtain a good result. We found that a simple, but effective option is to start from a current that radiates a field that complies with the requirements. This can be easily done by exploiting existing algorithms for the design of planar arrays (e.g. [10], [11]). In general, this current distribution is not achievable with a single source and a purely passive lossless impedance profile.

$$f(\mathbf{I}) = \alpha \sum_{i=1}^{N_{\text{cell}}} P_i(\mathbf{I})^2 + \beta \sum_{j=1}^{N_{\text{ff}}} \left(F_j(\mathbf{I}) - F_j^{\text{obj}}\right)^2 \tag{2}$$

$$P_i(\mathbf{I}) = \frac{1}{2} \operatorname{Re} \iint_{\mathcal{S}_i} \boldsymbol{E}(\mathbf{I}) \cdot \boldsymbol{J}_{\text{s}}(\mathbf{I})^* \, \mathrm{d}S \tag{3}$$

$$F_j(\mathbf{I}) = \left|\boldsymbol{E}_j(\mathbf{I}; \theta_j, \phi_j)\right|^2 \tag{4}$$

The objective function to be minimized (2) is formulated as the sum of two terms: the first one is the sum of the squared active power on each cell of the mesh (3), while the second one is the squared far field "magnitude error" (4) with respect to the objective field F^{obj}. The array $\mathbf{I}$ collects the RWG coefficients of the current.

In the summation, i runs across all the triangular cells, while j spans the far field directions in spherical coordinates (θ_j, ϕ_j). The values of the scaling factors α and β are chosen on a case-by-case basis.

This formulation leads to a non-convex optimization problem, which is tackled by means of a gradient descent algorithm: at each iteration, the gradient is computed and the function is minimized along the direction opposite to it. For large-size antennas, computing the gradient becomes the most computationally intensive step. Our formulation allows the objective function to be differentiated analytically and exploits fast algorithms for the computation of matrix-vector products, resulting in a overall complexity $O(N \log N)$. In particular, the GIFFT algorithm [12], [13] has been used in the computation of the scattered electric field.

The convergence criteria depends on the desired performance and usually involves the residual error being lower than a predefined relative tolerance. Once the optimization algorithm has converged, the resulting current coefficients $\mathbf{I}_{\text{opt}}$ are used to recover the impedance profile. To this aim, the unknown impedance is expanded with piecewise linear basis function on the node of the mesh, and the EFIE-IBC equation (5) is solved to find the coefficients of $\mathbf{Z}_{\text{s}}$,

$$\mathbf{Z}_{\text{s}}\mathbf{I}_{\text{opt}} = \mathbf{V}_{\text{inc}} + \mathbf{L}\mathbf{I}_{\text{opt}} \tag{5}$$

where $\mathbf{L}$ is the discretized operator that relates the current to the radiated field on the surface and $\mathbf{V}_{\text{inc}}$ is the field radiated by the source in absence of the surface impedance.

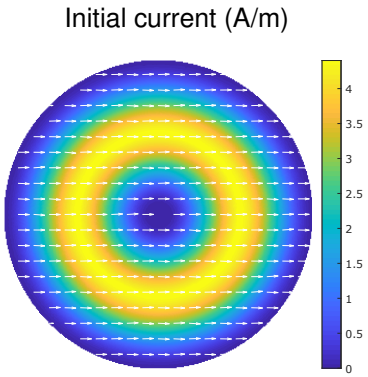

Fig. 1: Initial current used in the optimization process. It is a nearly uniform distribution polarized along the x direction, tapered toward the edges. Arrows represent the local direction of the current.

The resulting profile is then filtered to limit high frequency variations of the impedance and its residual real part is set to zero to avoid losses.

III. Results

A. Circular Metasurface Antenna

The algorithm has been applied to the design of a circular metasurface antenna working at a frequency of 32 GHz. It has a diameter $d = 55$ mm $\approx 6\lambda$ and is placed on a grounded dielectric slab with $\varepsilon_{\text{r}} = 3$ and thickness $h = 0.76$ mm. The antenna is fed by a vertical pin at the center, which excites a cylindrical TM surface wave. The surface was discretized with a triangular mesh with an average edge size of $\approx \lambda/10$ and the current was expanded with 24046 RWG basis functions. Given the large electrical size of the problem, the required matrix-vector products were accelerated as described in section II-B.

The objective far field was chosen as the one radiated by a nearly uniform current distribution polarized along the x

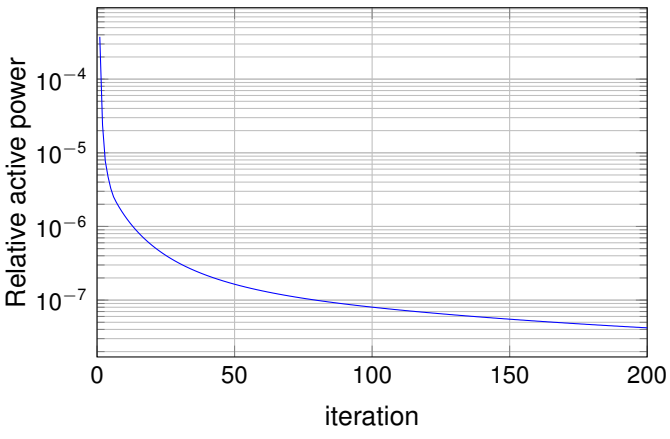

Fig. 2: Convergence of the iterative optimization algorithm. Values are computed as the ratio between the surface active power and the total radiated power.

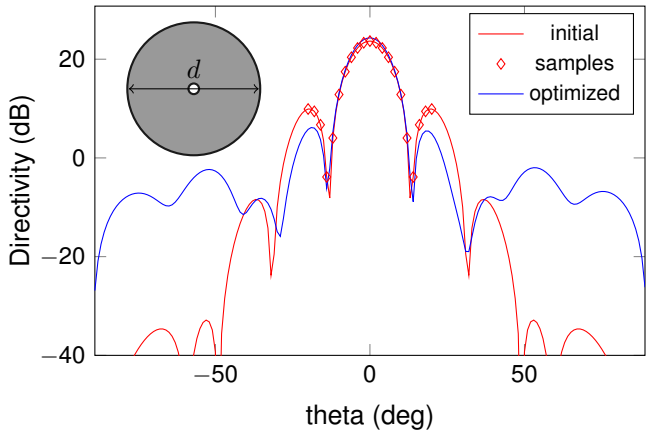

(a)

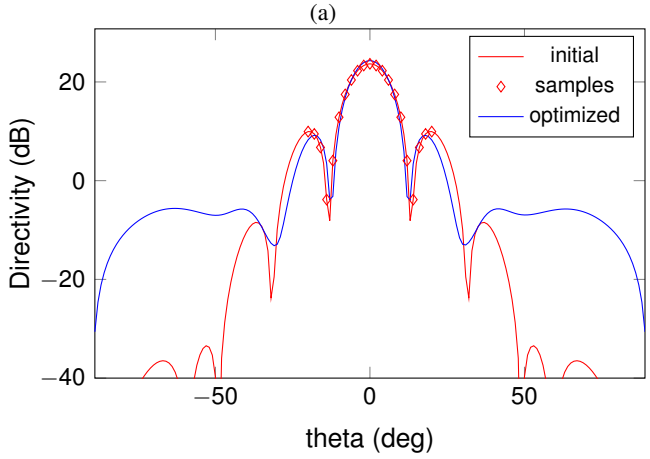

(b)

Fig. 3: Far field directivity pattern of the designed circular metasurface antenna: (a) $\phi = 0°$ cut, (b) $\phi = 90°$ cut. Initial field (solid red line), samples of the objective field used in the optimization (markers) and optimized far field (solid blue line).

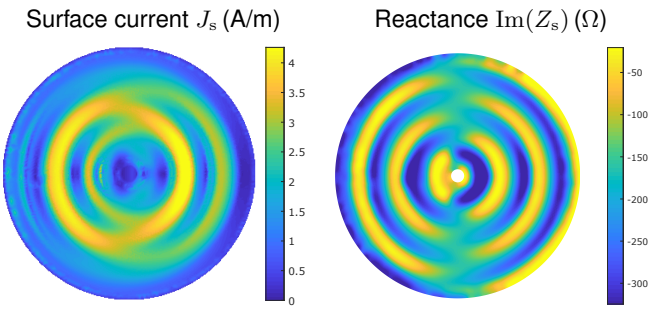

(a) (b)

Fig. 4: Designed circular metasurface antenna: (a) optimized surface current magnitude, (b) Imaginary part (reactance) of the surface impedance.

direction and tapered at the inner and outer edges (Fig. 1). This choice features a very high gain (almost the highest achievable given the size of the radiating aperture), with a broadside beam and low sidelobe levels. The far field sampling points were distributed on a regular grid around the broadside direction (up to $\theta = 20°$), with $N_\theta = 10$ and $N_\phi = 50$. The current that generates this field was also employed as the initial one in the optimization process. Scaling constants were set as to have the same order of magnitude for the two terms of the objective function ($\alpha = 1$ and $\beta = 1 \cdot 10^{-14}$). The optimization was set to stop once a relative improvement of 10^{-7} in the objective function is reached.

The stopping criteria was met after 200 iterations, which took around 30 s each, for a total running time of approximately 100 minutes. In Fig. 2, the convergence of the algorithm is represented with reference to the relative active power. The directivity pattern is shown in Fig. 3: in the main lobe region the agreement between the objective and synthesized far field is satisfactory. Outside this region, where samples were not included in the objective function, sidelobes are higher compared to the initial field. Fig. 4a shows the optimized current distribution, which is not symmetric due to the expected linear polarization of the objective field. Fig. 4b illustrates the resulting reactance profile, which has been filtered to smooth out high frequency variations. The residual real part of the impedance has been set to zero to ensure reactivity.

IV. Conclusions

A novel algorithm for the automated design of metasurface antennas has been presented. It focuses on the unconstrained optimization of the equivalent surface current distribution, from which a passive and lossless impedance is obtained at the end of the process. The algorithm takes into account the requirements of passivity and on the radiated field, without a priori assumptions on the current and impedance distributions. As such, it is general and can be efficiently combined with existing fast integral equation algorithms to accelerate the computation. It was tested by designing a circular metasurface antenna, with satisfactory results that support the effectiveness of the proposed approach.

Acknowledgment

This work was supported by the Italian Ministry of Research PRIN 2017S29ZLA “Metasurface Antennas for Space Applications”.

References

[1] M. Faenzi, G. Minatti, D. González-Ovejero, F. Caminita, E. Martini, C. D. Giovampaola, and S. Maci, “Metasurface Antennas: New Models, Applications and Realizations,” *Scientific Reports*, vol. 9, no. 1, pp. 1–14, Jul. 2019. [Online]. Available: https://www.nature.com/articles/s41598-019-46522-z

[2] A. M. Patel and A. Grbic, “Effective Surface Impedance of a Printed-Circuit Tensor Impedance Surface (PCTIS),” *IEEE Transactions on Microwave Theory and Techniques*, vol. 61, no. 4, pp. 1403–1413, Apr. 2013.

[3] G. Minatti, F. Caminita, E. Martini, M. Sabbadini, and S. Maci, “Synthesis of Modulated-Metasurface Antennas With Amplitude, Phase, and Polarization Control,” *IEEE Transactions on Antennas and Propagation*, vol. 64, no. 9, pp. 3907–3919, Sep. 2016.

[4] M. Bodehou, C. Craeye, and I. Huynen, "Electric Field Integral Equation-Based Synthesis of Elliptical-Domain Metasurface Antennas," *IEEE Transactions on Antennas and Propagation*, vol. 67, no. 2, pp. 1270–1274, Feb. 2019.

[5] M. Bodehou, C. Craeye, E. Martini, and I. Huynen, "A Quasi-Direct Method for the Surface Impedance Design of Modulated Metasurface Antennas," *IEEE Transactions on Antennas and Propagation*, vol. 67, no. 1, pp. 24–36, Jan. 2019.

[6] T. Brown, C. Narendra, Y. Vahabzadeh, C. Caloz, and P. Mojabi, "On the Use of Electromagnetic Inversion for Metasurface Design," *IEEE Transactions on Antennas and Propagation*, vol. 68, no. 3, pp. 1812–1824, Mar. 2020.

[7] T. Brown, Y. Vahabzadeh, C. Caloz, and P. Mojabi, "Electromagnetic Inversion With Local Power Conservation for Metasurface Design," *IEEE Antennas and Wireless Propagation Letters*, vol. 19, no. 8, pp. 1291–1295, Aug. 2020.

[8] M. Zucchi, F. Vernì, M. Righero, and G. Vecchi, "Automated Synthesis of Metasurface Antennas," in *Proc. of the 15th European Conference on Antennas and Propagation (EuCAP)*, May 2021.

[9] M. A. Francavilla, E. Martini, S. Maci, and G. Vecchi, "On the Numerical Simulation of Metasurfaces With Impedance Boundary Condition Integral Equations," *IEEE Transactions on Antennas and Propagation*, vol. 63, no. 5, pp. 2153–2161, May 2015.

[10] O. M. Bucci, G. Franceschetti, G. Mazzarella, and G. Panariello, "Intersection approach to array pattern synthesis," *Antennas and Propagation IEE Proceedings H - Microwaves*, vol. 137, no. 6, Dec. 1990.

[11] J. L. Araque Quijano and G. Vecchi, "Alternating Adaptive Projections in Antenna Synthesis," *IEEE Transactions on Antennas and Propagation*, vol. 58, no. 3, pp. 727–737, 2010.

[12] Fasenfest, Capolino, Wilton, Jackson, and Champagne, "A Fast MoM Solution for Large Arrays: Green's Function Interpolation With FFT," *IEEE Antennas and Wireless Propagation Letters*, vol. 3, pp. 161–164, 2004.

[13] S. M. Seo and J.-F. Lee, "A Fast IE-FFT Algorithm for Solving PEC Scattering Problems," *IEEE Transactions on Magnetics*, vol. 41, no. 5, pp. 1476–1479, 2005.